Unstructured grid large eddy simulation of wall bounded turbulent flows

By Kenneth Jansen

1. Motivation and objectives

Historically, large eddy simulations (LES) have been restricted to simple geometries where spectral or finite difference methods have dominated due to their efficient use of structured grids. Structured grids, however, not only have difficulty representing complex domains and adapting to complicated flow features, but also are rather inefficient for simulating flows at high Reynolds numbers. The lack of efficiency stems from the need to resolve the viscous sublayer which requires very fine resolution in all three directions near the wall. Structured grids make use of a stretching to reduce the normal grid spacing but must carry the fine resolution in the streamwise and spanwise directions throughout the domain. The unnecessarily fine grid for much of the domain leads to disturbingly high grid estimates. Chapman (1979), and later Moin & Jimenéz (1993), pointed out that, in order to advance the technology to airfoils at flight Reynolds numbers, structured grids must be abandoned in lieu of what are known as nested or unstructured grids. Figure 1 illustrates the ability of an unstructured mesh to refine only the near wall region. Note the large number of points near the wall (where the fine vortical features need better resolution) and the coarseness in all directions away from the wall (where the scales are much larger). The important difference between this approach and the usual structured grid stretching is that the number of elements used to discretize the spanwise and streamwise features of the flow is reduced in each successive layer coming off the wall. This is due to the fact that the elements not only grow in the normal direction, but in the other directions as well. This greatly reduces the total number of points or elements required for a given Reynolds number flow.

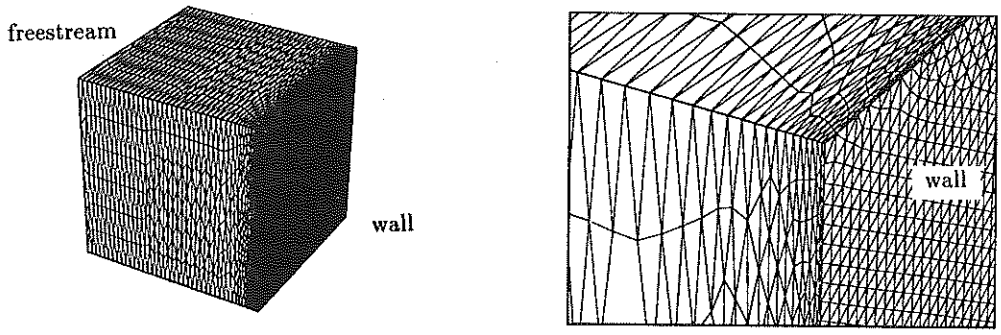

FIGURE 1. An unstructured grid places a large number of points at the wall but remains coarse in the freestream. The full mesh is shown in part (a) while a zoom of near wall corner is shown in part (b) to illustrate the refinement.

To estimate the number of unstructured grid elements required to simulate an airfoil, Chapman used flat plate skin friction analogies and a computational domain extending one-fifth chord in the spanwise direction to obtain

$$N = 0.2\frac{Re_c^{1.8}}{\Delta_x^+ \Delta_z^+} \tag{1}$$

where Δ_x^+ and Δ_z^+ are the grid resolutions in the streamwise and spanwise directions on the body surface and Re_c is the Reynolds number based on the chord, c and the freestream velocity, u_{inf}. This estimate assumes that the fine resolution near the wall is carried out for 10 layers to accurately resolve the viscous sublayer. Then, outside of the viscous sublayer, the elements grow rapidly in all three dimensions with increasing distance from the wall as described above. Moin & Jimenéz suggest that current subgrid-scale models should allow $\Delta_x^+ = 200$ and $\Delta_z^+ = 50$. When these values are substituted into (1), we observe that approximately 1.2×10^6 elements will be required for airfoils with a chord Reynolds number of $Re_c = 10^6$ and 80×10^6 elements for the more practical flight Reynolds number of $Re_c = 10^7$. Simulations of this scale are possible on today's supercomputers.

The use of unstructured grids, coupled with the advances in dynamic subgrid-scale modeling such as those made by Germano *et al.* (1991) and Ghosal *et al.* (1992), make LES of an airfoil tractable. The finite element method can efficiently solve the Navier-Stokes equations on unstructured grids. Although the CPU cost per time step per element is somewhat higher than structured grid methods, this effect is more than offset by the reduction in the number of elements.

2. Accomplishments

2.1 Computer code

The proposed finite element formulation is based on the work of Jansen *et al.* (1993), who used the method to model the compressible Reynolds-averaged Navier-Stokes equations. These simulations were performed by time marching a transient simulation to a steady solution. The code was optimized for rapid convergence without regard for time accuracy. For the current work, greater attention has been given to the efficient time accuracy before application to LES. Both explicit and implicit time integration methods have been developed and tested. Currently, the formulation has two implicit methods (first-order for acceleration towards a steady state and third-order for time accurate integration) and a higher order accurate family of explicit time integration methods.

2.2 Time step estimates

There is, in general, a tradeoff between explicit methods, which are cheaper per time step, and implicit methods, which require fewer time steps due to the avoidance of the stability limits. It can be shown through methods similar to Chapman's spatial estimate that the viscous stability limit leads to the following time step limit

$$\Delta_t^v = \frac{\Delta_y^+}{C_{f_{\max}} Re_c} T \tag{2}$$

where T is the time it takes the mean flow to cross the chord of the airfoil ($T = c/u_{\text{inf}}$) and $C_{f_{\max}}$ is the maximum of the coefficient of friction.

There is also a stability limit associated with advection. The time step associated with this stability limit is a little more difficult to estimate since it depends on both the mean flow advection, u, and the length of the element in the flow direction, Δ_s. These quantities vary throughout the flow. Assuming a logarithmic velocity profile and geometric stretching of the elements coming off the wall, it can be shown that the critical point occurs in the buffer layer near $y^+ = 10$. Respecting this advective stability limit leads to the following advective time step limit

$$\Delta_t^u = \alpha \Delta_t^v \tag{3}$$

where

$$\alpha \approx \frac{0.6\Delta_x^+}{\Delta_y^{+2}} \tag{4}$$

For the problem proposed above, $\Delta_x^+ = 200$ and Δ_y^+ is expected to be near 1.0, which makes $\alpha \approx 120$. This time step corresponds to a $\Delta_t^+ \approx 120$, which will not yield sufficient accuracy. Therefore, this stability limit is not likely to have any bearing on the size of the time step.

Since we are solving the compressible Navier-Stokes equations, a third time step restriction must be considered. The acoustic stability limit can be estimated as follows

$$\Delta_t^a = \beta \Delta_t^v \tag{5}$$

where

$$\beta = \frac{2.0M\sqrt{C_{f_{\max}}}}{\Delta_y^+} \tag{6}$$

where a is the acoustic speed and $M = u_{\text{inf}}/a$ is the freestream Mach number. Clearly, β is less than one, making this the most restrictive stability limit.

If Δ_y^+ is equal to one, it can be shown that Δ_t^v corresponds to a $\Delta_t^+ = 1.0$. Current channel flow LES simulations have had success with $\Delta_t^+ = 10.0$. Assuming that this temporal resolution is adequate for the airfoil, the acoustic time step stability limit will be far too restrictive. The implication of this result is that compressible formulations must provide an implicit treatment of the advective term. Furthermore, special care must be taken to show that the method is not adversely affected by simulating the flow at very high acoustic CFL numbers. For the conditions described above, typical flows lead to the following acoustic CFL estimate

$$\frac{a\Delta_t}{\Delta_x} = \frac{10.0}{\beta} \approx \frac{70.7}{M} \tag{7}$$

which exceeds 350 for a Mach number of 0.2.

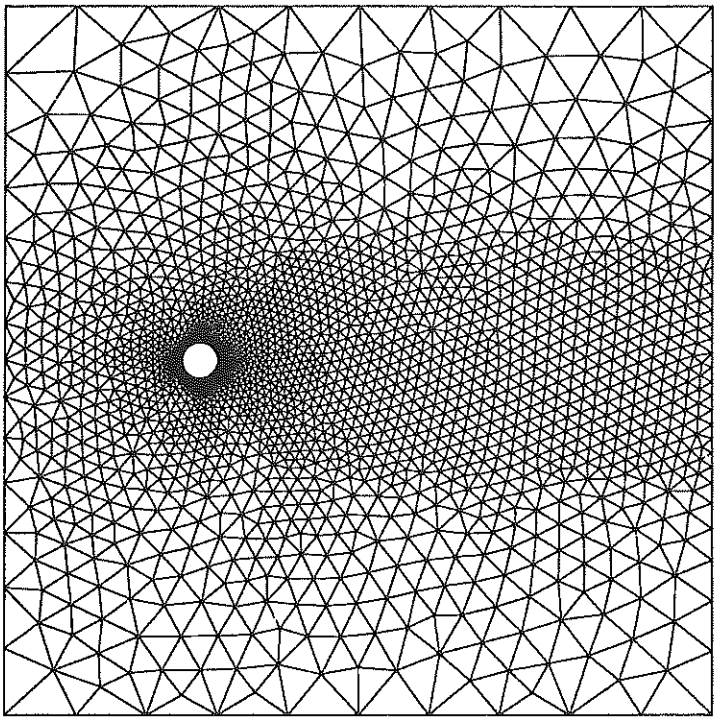

FIGURE 2. Unstructured grid for flow around a cylinder at $Re_d = 100$, $M = 0.2$. This mesh contains 4004 elements which corresponds to 2056 nodes for a linear space.

2.3 Preliminary simulations

To verify that the modifications to the code achieve time accuracy, the method was applied to laminar flow over a cylinder at $Re_d = 100, M = 0.2$. This flow leads to periodic vortex shedding and, therefore, gives some measure of a method's temporal-accuracy. The unstructured triangular mesh is shown in Figure 2. Note the local refinement near the cylinder and in the wake. The lift coefficient obtained by using piecewise linear shape functions in space and time can be seen in Figure 3. The Strouhal number for this discretization is 0.167. The acoustic CFL for this problem is 20.0.

3. Future plans

3.1 Time integration

The cylinder problem is not an adequate test of the formulation's ability to run at very high acoustic CFL numbers. A channel flow at a higher Reynolds will be run to determine the upper limit for the acoustic CFL number. Should problems arise, a change to an incompressible formulation may be appropriate. Such finite element formulations are currently being used by Hauke & Hughes (1993) and Simo

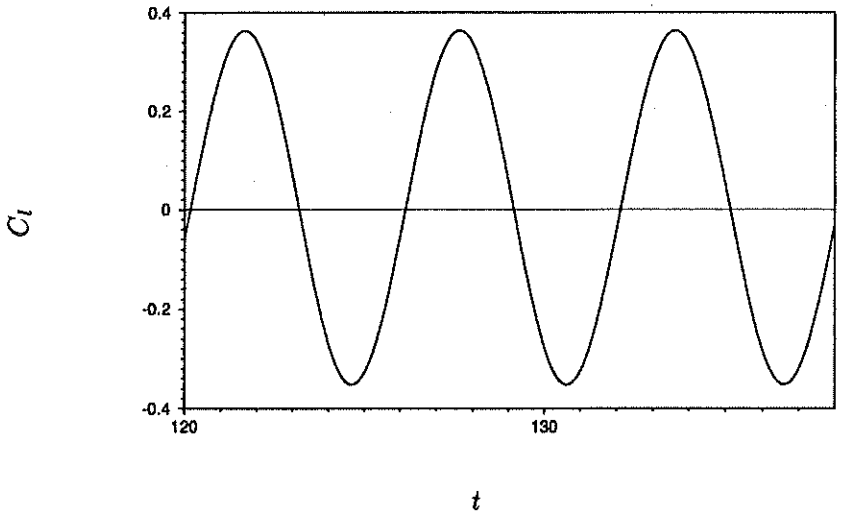

FIGURE 3. Periodic vortex shedding illustrated through the lift coefficient.

& Armero (1993) for laminar flows. The drawback to an incompressible formulation is that many interesting airfoil problems require the consideration of compressibility effects.

3.2 Mesh generation

The mesh requirements of the airfoil problem exceed existing mesh generation capability. In order to stretch the elements to the level described above and to reduce the number of elements with distance from the wall, new mesh generation techniques must be developed. It is crucial that elements do not have angles which approach 180°. An algorithm to accomplish this goal for airfoils is under development in collaboration with Tim Barth of NASA Ames. This algorithm also should provide smoother element shape changes than those observed in Figure 1, resulting in higher quality solutions.

3.3 Subgrid-scale modeling

The dynamic models developed at CTR need to be implemented into the unstructured grid code. This is not expected to be too difficult, especially for higher order elements which have a built-in test grid (the corner nodes).

3.4 Further speeding up of the code

The code has been largely optimized for marching to steady state solutions. It may be possible to further optimize the code for time accurate calculations. The code currently runs at 440 MFLOPS on the Cray C90 and 25 MFLOPS per processor on the Thinking Machines CM5. These execution rates are quite fast, but some savings in the number of FLOPS per time step per element may be attainable.

9.5 Airfoil simulation

Upon the successful completion of these tasks, the code will be applied to airfoil problems with the ultimate target being airfoils at or near maximum lift; see Coles and Wadcock (1979). These flows commonly have separation bubbles that are difficult to predict with Reynolds-averaged Navier-Stokes equation models and, therefore, present an opportunity to demonstrate the utility of LES approaches.

REFERENCES

CHAPMAN, D. R. 1979 Computational aerodynamics development and outlook. *AIAA J.* **17,** 1293.

COLES, D., & WADCOCK, A. J. 1979 A flying-hot-wire study of two-dimensional mean flow past an NACA 4412 airfoil at maximum lift. *AIAA J.* **17,** 321.

GERMANO, M., PIOMELLI, U., MOIN, P. & CABOT, W. H. 1991 A dynamic subgrid-scale eddy viscosity model. *Phys Fluids A.* **3,** 1760.

GHOSAL, S., LUND, T. S. & MOIN, P. 1992 A dynamical localization model for large eddy simulation of turbulent flows. *CTR Manuscript 139.*

HAUKE, G., & HUGHES, T. J. R. 1993 A unified approach to compressible and incompressible flows. *Comp. Meth. Appl. Mech. Eng.* To appear.

JANSEN, K., JOHAN, Z., & HUGHES, T. J. R. 1993 Implementation of a one-equation turbulence model within a stabilized finite element formulation of a symmetric advective-diffusive system. *Comp. Meth. Appl. Mech. Eng.* **105,** 405.

MOIN, P. & JIMENÉZ, J. 1993 Large eddy simulation of complex turbulent flows. *AIAA-03-3099,* AIAA 24th Fluid Dynamics Conference.

SIMO, J. C., & ARMERO F. 1993 Unconditional stability and long term behavior of transient algorithms for the incompressible Navier-Stokes and Euler equations. *Comp. Meth. Appl. Mech. Eng.* To appear.